ISSN (Print) 1226-1750
ISSN (Online) 2233-6656
Journal of Magnetics 25(1), 15-21 (2020) https://doi.org/10.4283/JMAG.2020.25.1.015

Analysis of Magnetic Particle Agglomeration Structure and Interaction Forces Between Magnetic Particles

Jia Long[1], Zixu Miao[1], Huihuang Chen[2], Rongdong Deng[1], Weiran Zuo[1], Bao Guo[1], and Jiangang Ku[1,3]*

[1]College of Zijin Mining, Fuzhou University, Fuzhou 350116, Fujian, China
[2]School of Chemical Engineering, The University of Queensland, Brisbane, QLD 4072, Australia
[3]Fuzhou University-Zijin Mining Group Joint Research Center for Comprehensive Utilization of Mineral Resources, Fuzhou 350116, China

(Received 7 November 2019, Received in final form 10 January 2020, Accepted 14 January 2020)

Chain-like and diamond-shaped magnetic particle agglomeration (MPA) commonly forming in a weak magnetic field are simulated based on the finite element method (FEM), and the effects of particle diameter, magnetic field strength, particle relative magnetic permeability, and particle number in magnetic particle chains (MPCs) and diamond-shaped MPA on the strength of MPA are analysed in detail. The results show that magnetic forces on the centre contact points (CCPs) of MPA are positively correlated with the particle diameter, magnetic field strength, particle relative magnetic permeability, and particle number. In addition, the forces on the CCPs of the MPCs (N=2) have a square relationship with the particle diameter and magnetic field strength and have a power relationship of 1.25 with the particle relative magnetic permeability. The forces on each contact point decrease slowly from the centre to both ends in the MPCs and then rapidly decrease to one value (approximately 0.779 times the forces on the CCPs). As for the diamond-shaped MPA, with the increase in the angle α between the magnetic field and axis of diamond-shaped MPA, the force magnitude of the particle entrained parallelly in the diamond-shaped MPA shows a trend of a "cosine curve" shape and the minimum value is 2109 times that of the entrained particle's gravity. The angle θ between the direction of the force and the negative X-axis shows a trend of a "sine curve" shape. When α = 25° and 155°, the angle θ of the force on the entrained particle reaches an extreme value, that is, θ = 21.87°. Only if the angle θ reaches 30° can the particle entrained parallelly escape from the diamond-shaped MPA. Thus, the diamond-shaped MPA remains in a stable state and it is difficult to disperse MPA by changing the direction of the magnetic field.

Keywords : magnetic particle agglomeration, finite element method, simulation, forces analysis

1. Introduction

Magnetic particle agglomeration (MPA) [1] is a common physical phenomenon in the magnetic separation process. Once MPA encloses non-magnetic minerals such as gangue, the separation efficiency and concentrate index will be affected. In the process of magnetic separation, the core issues of magnetic separation research are reasonable utilisation of MPA without non-magnetic inclusions, effective destruction of MPA with non-magnetic inclusions, and reduction of non-magnetic mineral content in MPA [2]. At present, there are few studies on the structure of MPA and the interaction forces between internal magnetic particles.

The formation mechanism of MPA has been increasingly studied [3-5]. On the one hand, the interaction between magnetic particles in an applied magnetic field is the key to the study of the mechanism of MPA [6]. Under the action of an external magnetic field, the magnetic particles are not only affected by gravity, buoyancy, van der Waals force and Coulomb force, but also subject to the magnetic forces on magnetic particles and the interaction forces between magnetic particles. At first, the study about the interaction between magnetic particles was mainly based on the theory of magnetism [7], magnetic dipole theory [8], Coulomb's law [9], electromagnetic theory and molecular current hypothesis [10], and then the interaction between particles themselves by a numerical simulation method. Although the interaction between magnetic particles can be effectively calculated based on magnetic

©The Korean Magnetics Society. All rights reserved.
*Corresponding author: Tel: +86-150-8009-3186
Fax: +86-0591-22865213, e-mail: kkcc22@163.com

© 2020 Journal of Magnetics

theory [7], Coulomb's law [9], and binding strength formula [11, 12] under an external magnetic field, the interaction between magnetic dipoles will change the anisotropy of magnetic particles which can affect the magnetization process of the magnetic particles and change the magnetic agglomeration process [8]. The interaction between the magnetic dipole and magnetic dipole force on particles has an important influence on the magnetic separation process. However, with the further research, it is found that the magnetic dipole theory is not suitable for the magnetic agglomeration process with small distance between particles, so the numerical simulation of the magnetic particle agglomeration process based on the finite element method (FEM) has been widely used [13]. Zhao [13] used FEM to calculate the forces between magnetic particles and compared the results with those results calculated by a simplified magnetic dipole model and a non-simplified magnetic dipole model. Using FEM to calculate the shear yield force of magnetic particle single chain was more accurate. On the other hand, the research on the process of MPA will help to understand the mechanism of MPA [14]. Volkova [15] studied micron-sized magnetic polystyrene particles and analysed the formation process of magnetic particle chain (MPC) under an external magnetic field. Sheng [16] placed a number of ferromagnetic glass balls in external magnetic and electric fields. The experimental results found that the balls formed a cylindrical chain structure in the fields and the process and structure of MPC formation under different fields was basically the same. In addition, these studies show that the agglomeration process of magnetic particles is often affected by magnetic particle properties, magnetic particle diameter [17], magnetic particles permeability [18], and magnetic field strength [19, 20]. Cernak [19] studied the formation and growth of acicular agglomerations in magnetic fluid films in a magnetic field and found the magnetic field strength was a key factor affecting the average length of the agglomerations. Ku *et al.* [21, 22] established an MPA dynamics model of macroscopic particle groups, calculated various forces of ore groups in a magnetic field, and found that the forces between magnetic dipoles and viscous drags were major factors affecting MPA on the basis of the magnetic field distribution theory.

Most of the aforementioned studies on the interaction

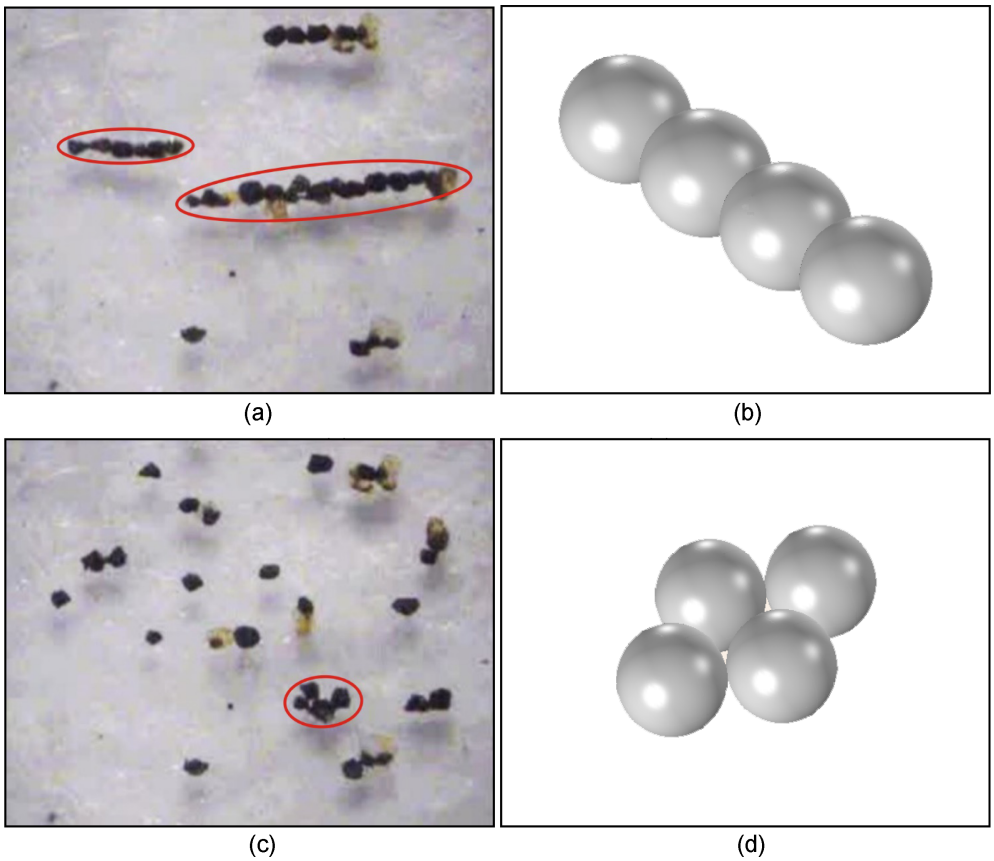

Fig. 1. (Color online) Three-dimensional geometric models of MPA. (a) Magnetic mineral particles appearing chain-like in a magnetic field. (b) Model of MPC; (c) Magnetic mineral particles appearing diamond-shaped in a magnetic field. (d) Model of diamond-shaped MPA.

forces between magnetic particles adopted magnetic dipole theory, but when the distance of magnetic particles decreases, some large errors will occur while calculating the interaction forces between particles using the magnetic dipole model [23, 24]. In this paper, based on FEM, a more accurate near-field analysis method, three-dimensional (3D) geometric models of chain-like and diamond-shaped MPA are established, forces on the contact points inside chain-like and diamond-shaped MPA are calculated, the stability of diamond-shaped MPA is discussed, and a theoretical basis for related research into magnetic separation theories and magnetic separation equipment is provided.

2. Magnetic Particle Agglomeration Geometric Model And Simulation Parameters

FEM software COMSOL Multiphysics (version 5.3a) was used to establish three-dimensional geometric models of chain-like and diamond-shaped MPA, as shown in Fig. 1.

2.1. Magnetic particle chain

In the MPC model, magnetic fields of different strengths are applied along the Y-axis direction. The relevant simulation parameters are shown in Table 1.

2.2. Diamond-shaped magnetic particle agglomeration

In the diamond-shaped MPA model, magnetic fields of different angles are applied on the X-Y plane. The relevant simulation parameters are shown in Table 2.

3. Solution Region and Solving the Equation of Models

The closed field surrounding particles is divided into finite meshes. The function of the whole field is discretised, a set of approximate algebraic equations are obtained, and the approximate values of the field function are acquired by solving these equations simultaneously. In this paper, the finite element function of the models is solved using COMSOL Multiphysics (version 5.3a).

3.1. Solution region and mesh generation

The 3D geometric models constructed in this paper can be regarded as a magnetic particle-water system, in which a magnetic field is applied. To eliminate the influence of the boundary conditions on the calculation results of the models, the water body size (Lx=Ly=Lz=35 mm) is set to be much larger than the magnetic particle diameters. Considering the influence of magnetic coupling and edge effects, the physical parameters and simulation results of MPA (chain-like and diamond-shaped) in the magnetic field are obtained by solving those functions. MPA is divided into free tetrahedron elements using free mesh generation technology. The 3D geometric structure of the magnetic particles is expressed in the form of nodes and units. To solve the equations of several discrete units and obtain accurate simulation results, the paper properly set the maximum and minimum mesh sizes of the free tetrahedral meshes and the mesh element sizes are very small and the qualities of these meshes are very good in

Table 1. Simulation parameters.

Parameter name	Symbol	Unit	Value
Magnetic field intensity	H	T	0.1, 0.125, 0.15
Magnetic particle diameter	d	mm	0.05, 0.1, 0.2
Magnetic particle density	ρ	Kg/m^3	5200
Particles' relative magnetic permeability	u_r	1	1.05, 2, 3, 4, 5.16
Magnetic permeability in vacuum	u_0	Wb/(m·A)	$4\pi \times 10^{-7}$
Particle number	N		2, 4, 8, 16

Table 2. Simulation parameters.

Parameter name	Symbol	Unit	Value
Magnetic field intensity	H	T	0.125
Magnetic particle diameter	d	mm	0.1
Magnetic particles density	ρ	Kg/m^3	5200
Particles' relative magnetic permeability	u_r	1	5.16
Magnetic permeability in vacuum	u_0	Wb/(m·A)	$4\pi \times 10^{-7}$
Particle number	N		4
Deflection angle of magnetic field	α	°	0, 15, 30, 45, 60, 75, 90, 105, 120, 135, 150, 165, 180

The angle α is between the magnetic field and the axis of the diamond-shaped MPA on the X-Y plane.

this paper.

3.2. Solving the equation

(1) The water body region and magnetic particles satisfy the equation of magnetic flux conservation:

$$\nabla \cdot B = 0 \tag{1}$$

$$H = -\nabla V_m \tag{2}$$

The constitutive relationship of the magnetic field in the water body region is as follows:

$$B = \mu_0 \mu_r H + B_r \tag{3}$$

The constitutive relationship of the magnetic particles in the magnetic field is as follows:

$$B = \mu_0 (H + M), \tag{4}$$

where ∇ is the Hamiltonian operator, B is the magnetic induction or magnetic flux density, H is the magnetic field intensity, V_m is the magnetic vector potential, $V_m = 0$ or zero magnetic potential, μ_0 is the magnetic permeability in vacuum, $\mu_0 = 4\pi \times 10^{-7}$ Wb/(m·A), B_r is the residual magnetic induction or the residual magnetic intensity flux density, μ_r is the particle relative magnetic permeability, and M is the intensity of the magnetisation of the magnetic particles.

(2) The magnetic insulation equation is:

$$n \cdot B = 0, \tag{5}$$

where n is the boundary normal vector.

(3) The force calculation equation of the magnetic particles is:

$$F = \int_{\partial\Omega} nTds \tag{6}$$

$$\tau = \int_{\partial\Omega} (r - r_0) \times (nT) ds \tag{7}$$

$$\tau_{ax} = \frac{r_{ax}}{|r_{ax}|} \cdot \tau, \tag{8}$$

where F is the force of the magnetic particles in the magnetisation field, n is the magnetic particle boundary normal vector, T is the torque, ds is an area element on the surface of one magnetic particle, τ is the magnetic particle volume, τ_{ax} is the magnetic particle volume axis, r is the magnetic particle position, r_0 is the magnetic particle torque rotation point, and r_{ax} is the magnetic particle torque shaft.

4. Calculation Results and Discussion

4.1. Forces on different contact points in MPCs

4.1.1. Forces on the centre contact points (CCPs) in MPCs

In a magnetic field, the magnetic forces on the CCPs (the contact point on the surface of one particle contacts another which is in the center of the magnetic particle chain) are related to the particle diameter, magnetic field strength, particle relative magnetic permeability, and particle number. In MPCs composed of different magnetic particle diameters, particle relative magnetic permeabilities, and particle numbers, the relationships between the forces acting on the CCPs in the MPCs and magnetic field strength are shown in Fig. 2. Fig. 2 demonstrates that the forces on the CCPs of the MPCs increase with the increase in the particle diameter, magnetic field strength, and particle relative magnetic permeability. Meanwhile, the forces acting on the CCPs increase rapidly at first and then increase slowly until reaching a stable value with the increase in the particle number. When the particle number of an MPC increases from 2 to 4 and 8, the force on the CCP increases by 1.142-1.725 times and 1.032-1.035 times respectively. When the particle number increases to 16, the force changes slightly.

By analysing the relationship between the forces on the CCPs in the MPCs (particle number N=2) and particle diameter (see Fig. 3), the theoretical formula describing the forces on the CCPs in the MPCs and particle diameter, magnetic field strength, and particle relative magnetic permeability is:

$$F = 1500000 \times u_r^{1.25} d^2 H^2 \tag{9}$$

The formula demonstrates that the forces on the CCPs in the MPCs (N=2) have a 1.25-power relationship with the particle relative magnetic permeability and a 2-power

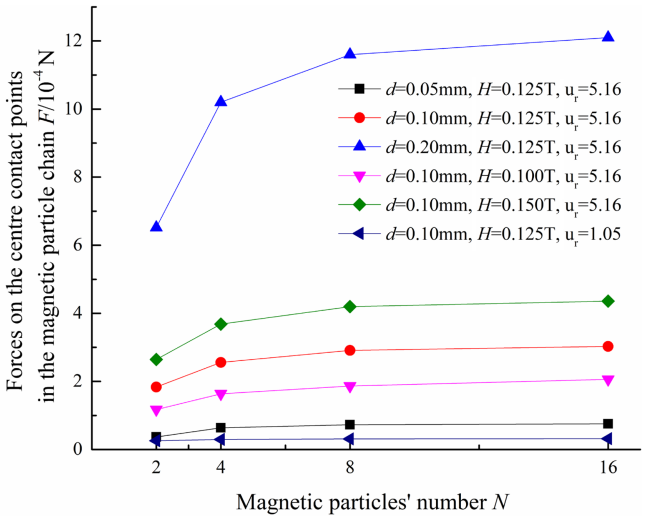

Fig. 2. (Color online) Forces on the centre contact points in magnetic fields.

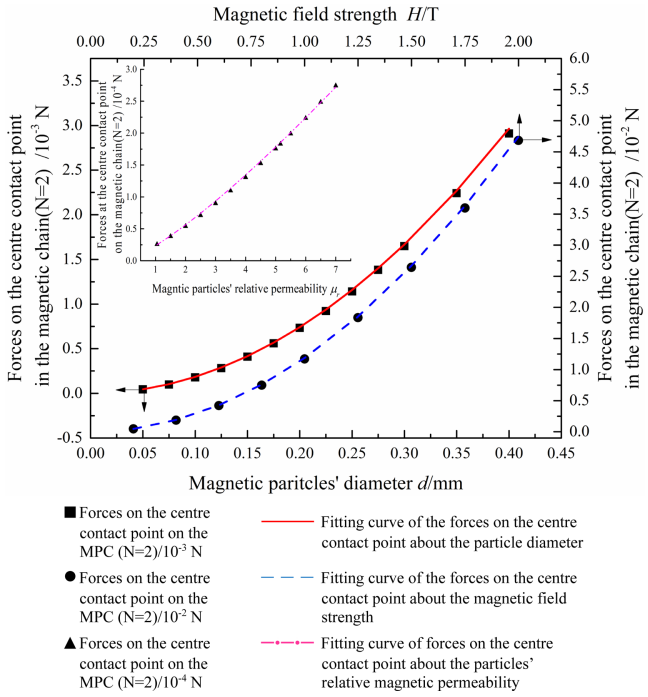

Fig. 3. (Color online) Fitting curve of the central contact point's forces on MPCs (N=2) with different particle diameters.

relationship with the particle diameter and magnetic field strength, respectively. Meanwhile, the data obtained by the formula fit well with the forces on the CCPs and the fitting degree is over 0.9935.

4.1.2. Forces on different contact points in MPCs

It is assumed that forces on each contact point in the MPC along the Y-axis from the centre forward is $f_0, f_1, \cdots, f_n$ (in which n = N/2-1, n is the order of contact points from the center to the outside in the magnetic particle chain). The relationships between the forces on the different contact points and the particle diameter, magnetic field strength, and particle relative magnetic permeability in the MPC (N=4) are shown in Fig. 4. Fig. 4 demonstrates that the value of f_1/f_0 decreases with the increase in the particle relative magnetic permeability but is less affected by the particle diameter and magnetic field strength. Under different conditions, the value of f_1/f_0 is less than 1, that is, the forces gradually decrease from the centre to the end of the MPC. When the particle diameter is 0.1 mm, the particle relative magnetic permeability is 5.16 and the magnetic field strength is 0.125 T. The relationships between the forces on each contact point in the MPC and particle number is shown in Fig. 5. Fig. 5 demonstrates that the variation law of the forces on each contact point is similar to that when the particle number is

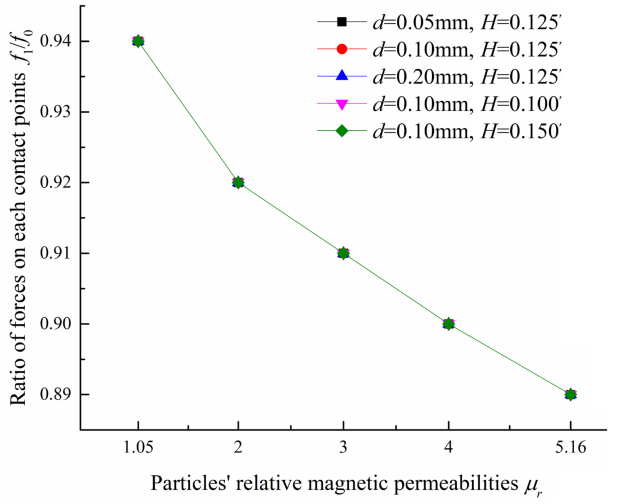

Fig. 4. (Color online) Forces on each contact point in MPCs (N=4).

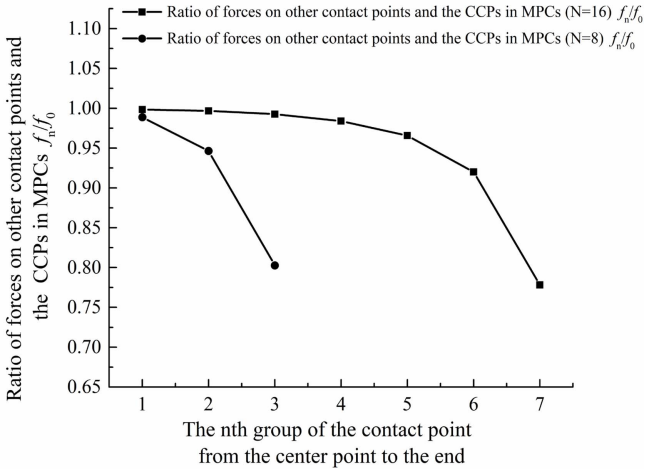

Fig. 5. Force ratio between contact points and magnetic particles in MPCs (N=8 and 16).

4 in the MPC. When the particle number is 16, the value of f_1/f_0 decreases slowly from 0.99 at first and then decreases rapidly. The forces on the far end in the MPC are approximately 0.779 times that of the CCPs. When the particle number is 8, the trend in the change is more obvious.

4.2. Stability of diamond-shaped magnetic particle agglomeration (diamond-shaped MPA)

Since the diamond-shaped MPA is a symmetrical structure, the force acting on particle C entrained parallelly in the diamond-shaped MPA is analysed (see Fig. 6). The relationship between the force's magnitude and the direction on particle C and different deflection angles of the magnetic field is shown in Fig. 6. Fig. 6 demonstrates that as the angle α that is between the magnetic field direction

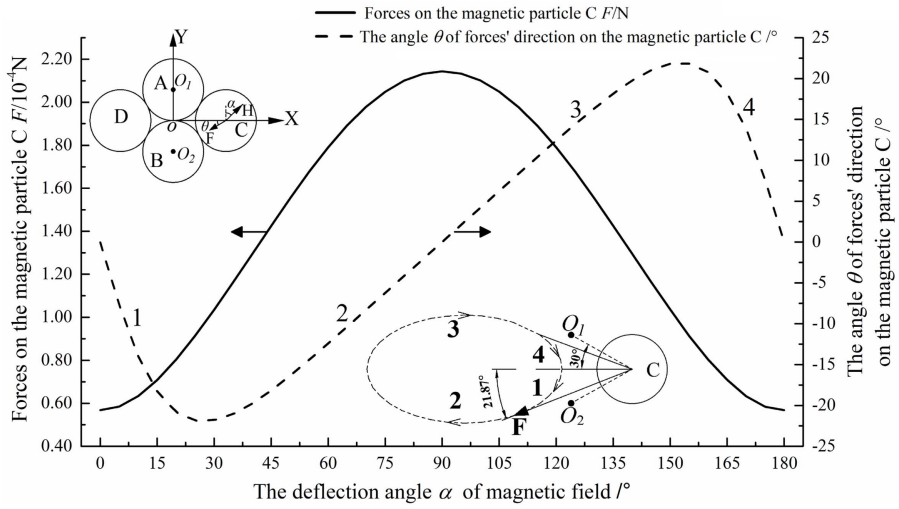

A, B, C, and D represent the magnetic particles in the diamond-shaped magnetic particle agglomeration respectively. O_1 and O_2 represent the centre of magnetic particle A and B respectively. α is the angle between the magnetic field and the axis of the diamond-shaped MPA and θ is the angle between the forces' direction on particle C and the X axis.

Fig. 6. Forces on particle C of diamond-shaped magnetic aggregates under a magnetic field.

and the axis of the diamond-shaped MPA increases from 0º to 180º, the magnitude of the force on the particle C shows a trend of a "cosine curve" shape and the force's magnitude variation range is 5.68×10^{-5}–2.14×10^{-3} N. The angle θ, the value of the direction of the force on particle C that is between the forces' direction on particle C and the negative X-axis shows a trend of a "sine curve" shape and a variation range of θ is 0°–21.87°. When α = 0° and 180°, the forces on particle C are the smallest (approximately 2109 times that of particle C's gravity). When $\alpha = 90°$, the force on particle C is the largest (up to 7961 times that of particle C's gravity). When $\alpha = 25°$ and 155°, the angle θ reaches an extreme value, that is, $\theta = 21.87°$, and the force magnitude is 9.14×10^{-5} N (approximately 3394 times that of particle C's gravity). However, only if the angle θ reaches 30º can particle C entrained parallelly escape from the diamond-shaped MPA. Thus, the diamond-shaped MPA remains in a stable state and it is difficult to disperse MPA by changing the direction of the magnetic field.

5. Conclusion

In a magnetic field, forces on each contact points in MPA are quite different and affected by magnetic particles' own properties and magnetic field. And it is found that it is difficult to disperse MPA by changing the direction of the magnetic field unless the angle θ reaches 30º in the diamond-shaped MPA.

Acknowledgements

This work was financially supported by the National Natural Science Foundation of China (Grant No. 51674091 and 51604084) and the Natural Science Foundation of Fujian Province of China (Grant No. 2017J01483), and National Training Program of Innovation and Entrepreneurship for Undergraduates (Grant No. 201810386029).

References

[1] Z. T. Yuan, L. X. Li, and Q. Feng, Questions and Answers on Magnetoelectricity Beneficiation Technology (2012).
[2] L. Z. Chen, J. W. Zeng, C. P. Guan, H. F. Zhang, and R. Y. Yang, Miner. Eng. **78**, 122 (2015).
[3] N. Eibagi, J. J. Kan, F. E. Spada, and E. E. Fullerton, IEEE Magn. Lett. **3**, 4500204 (2012).
[4] M. Kaur, H. J. Zhang, and Y. Qiang, IEEE Magn. Lett. **4**, 4000204 (2013).
[5] L. Z. Chen, W. B. Liu, J. W. Zeng, and P. Ren, Powder Technol. **313**, 54 (2017).
[6] J. G. Ku, W. B. Zhang, and D. W. Liu, Metal Mine. **6**, 30 (2007).
[7] Y. M. Eyssa and R. W. Boom, Int. J. Miner. Process. **3**, 1 (1976).
[8] D. Fletcher, IEEE Trans. Magn. **27**, 5375 (1991).
[9] Y. M. Wang, R. J. Pugh, and E. Forssberg, Colloids Surf. A. **90**, 117 (1994).
[10] C. Lin, C. Y. Sun, and J. M. Xu, Min. Meta. **9**, 1 (2000).
[11] E. M. Furst and A. P. Gast, Phys. Rev. E. **61**, 6732 (2000).

[12] Q. Xie, Metallic. Ore. Dress. Abroad. **37**, 2 (2000).
[13] C. W. Zhao and X. H. Peng, J. Func. Mater. **43**, 15 (2012).
[14] R. S. Miao and S. C. Saxena, Powder Technol. **86**, 187 (1996).
[15] O. Volkova, S. Cutillas, P. Carletto, G. Bossisa, A. Cebersb, and A. Meuniera, J. Magn. Magn. Mater. **201**, 66 (1999).
[16] P. Sheng, W. J. Wen, N. Wang, H. R. Ma, Z. F. Lin, W. Y. Tam, and C. T. Chan, Phys. B: Cond. Matt. **279**, 168 (2000).
[17] C. Tsouris and T. C. Scott, Colloid Polym. Sci. **171**, 319 (1995).
[18] J. Popplewell and R. E. Rosensweig, J. Phys. D: Appl. Phys. **29**, 2297 (1996).
[19] J. Cernak, P. Macko, and M. Kasparkova, J. Phys. D: Appl. Phys. **24**, 1609 (1991).
[20] H. A. Garcia-Martinez, M. Llamas-Bueno, S. X. Song, and A. Lopez-Valdivieso, Miner. Process. Extra. Metall. Rev. **25**, 67 (2004).
[21] J. G. Ku, H. H. Chen, K. He, and Q. X. Yan, J. Central South University **46**, 5 (2015).
[22] J. G. Ku, H. H. Chen, K. He, and Q. X. Yan, Miner. Eng. **79**, 10 (2015).
[23] J. G. Ku, X. Y. Liu, H. H. Chen, R. D. Deng, and Q. X. Yan, AIP Adv. **6**, 025004 (2016).
[24] D. Du, F. Toffoletto, and S. L. Biswal, Phys. Rev. E Stat. Nonlin Soft Matter Phys. **89**, 4 (2014).